Geoderma 313 (2018) 25–40

Contents lists available at ScienceDirect

Geoderma

journal homepage: www.elsevier.com/locate/geoderma

Open digital mapping as a cost-effective method for mapping peat thickness and assessing the carbon stock of tropical peatlands

Rudiyanto[a,*], Budiman Minasny[b,*], Budi Indra Setiawan[a,*], Satyanto Krido Saptomo[a], Alex B. McBratney[b]

[a] Department of Civil and Environmental Engineering, Bogor Agricultural University, Kampus IPB Darmaga, PO Box 220, Bogor 16002, Indonesia
[b] Sydney Institute of Agriculture, School of Life and Environmental Sciences, The University of Sydney, 1 Central Avenue, Australian Technology Park, Eveleigh, NSW 2015, Australia

ARTICLE INFO

Handling Editor: Morgan Crisitne L.S.

Keywords:
Tropical peatlands
Carbon stock
Digital soil mapping
Machine-learning
Climate change
Open-source

ABSTRACT

Tropical peatland holds a large amount of carbon in the terrestrial ecosystem. Indonesia, responding to the global climate issues, has legislation on the protection and management of the peat ecosystem. However, this effort is hampered by the lack of fine-scale, accurate maps of peat distribution and its thickness. This paper presents an open digital mapping methodology, which utilises open data in an open-source computing environment, as a cost-effective method for mapping peat thickness and estimating carbon stock in Indonesian peatlands. The digital mapping methodology combines field observations with factors that are known to influence peat thickness distribution. These factors are represented by multi-source remotely-sensed data derived from open and freely available raster data: digital elevation models (DEM) from SRTM, geographical information, and radar images (Sentinel and ALOS PALSAR). Utilising machine-learning models from an open-source software, we derived spatial prediction functions and mapped peat thickness and its uncertainty at a grid resolution of 30 m. Peat volume can be calculated from the thickness map, and based on measurements of bulk density and carbon content, carbon stock for the area was estimated. The uncertainty of the estimates was calculated using error propagation rules. We demonstrated this approach in the eastern part of Bengkalis Island in Riau Province, covering an area around 50,000 ha. Results showed that digital mapping method can accurately predict the thickness of peat, explaining up to 98% of the variation of the data with a median relative error of 5% or an average error of 0.3 m. The accuracy of this method depends on the number of field observations. We provided an estimate of the cost and time required for map production, i.e. 2 to 4 months with a cost between $0.3 and $0.5/ha for an area of 50,000 ha. Obviously, there is a tradeoff between cost and accuracy. The advantages and limitations of the method were further discussed. The methodology provides a blueprint for a national-scale peat mapping.

1. Introduction

Tropical peatland plays an important role in the global carbon cycle as it stores a large amount of carbon in the terrestrial ecosystem (Mitra et al., 2005). Carbon stored in peatland can be 10 times larger than its aboveground biomass (Draper et al., 2014; Rudiyanto et al., 2016a). Peatland in Indonesia was considered as marginal land and as a fuel resource prior to the year 2000 (Supardi et al., 1993). With increasing awareness of peat's large C stock and potential greenhouse gases emission (Comeau et al., 2016), accurate estimation of carbon stock of tropical peatlands becomes an important issue (Warren et al., 2017). In addition, carbon stock estimation in peatland is required to support carbon emission reduction policies (Page et al., 2011).

Indonesia, responding to the global issue of reducing CO_2 emissions, has legislation on the protection and management of the peat ecosystem. The legislation outlined conservation areas, which depends on the thickness of peat; however, the main challenge is the lack of fine-scale, accurate maps of peat distribution and its thickness. The current peatland map in Indonesia is at 1:250,000 scale with an estimated area of 14.9 million ha in Sumatra, Kalimantan and Papua (Ritung et al., 2011; Wahyunto and Subagjo, 2003; Wahyunto and Subagjo, 2004; Wahyunto et al., 2006). However there is still much uncertainty in this map (Hooijer and Vernimmen, 2013; Warren et al., 2017), and this coarse scale map cannot be used to implement conservation and management regulations.

Traditional soil mapping techniques are too costly as they require

* Corresponding authors.
E-mail addresses: lupusae@yahoo.com (Rudiyanto), budiman.minasny@sydney.edu.au (B. Minasny), budindra@ipb.ac.id (B.I. Setiawan).

http://dx.doi.org/10.1016/j.geoderma.2017.10.018
Received 9 August 2017; Received in revised form 6 October 2017; Accepted 16 October 2017
Available online 06 November 2017

many field observations, and the outputs can be too subjective. Many technologies for mapping peatlands have been tested in Indonesia, including remote-sensing technologies that monitor soil from the above (e.g. ICCC, 2014; Ritung et al., 2011; Shimada et al., 2016). However many of those technologies are not cost-effective for large extent mapping. This paper aims to demonstrate and validate a digital mapping methodology, which utilises open data in an open-source environment, as a cost-effective and accurate method for mapping peat thickness and estimating carbon stock for a large extent area.

Considerable attempts have been carried to develop methods that produce accurate maps of peat thickness. Kriging interpolation is often used (Akumu and McLaughlin, 2014; Altdorff et al., 2016; Bauer et al., 2003; Jaenicke et al., 2008; Keaney et al., 2013; Proulx-McInnis et al., 2013; van Bellen et al., 2011; Weissert and Disney, 2013); however to produce a fine resolution map, it needs a large number of observations evenly spread throughout the area. Spatial models were also used to predict peat thickness, such as regression analysis from terrain attributes (e.g., elevation and slope) (Holden and Connolly, 2011; Parry et al., 2012); a peat thickness inference model (Holden and Connolly, 2011); a power function of the distance to a river (Hooijer and Vernimmen, 2013); an exponential function of elevation and slope (Parry et al., 2012); an empirical function of elevation (Rudiyanto et al., 2015). These models only consider few environmental factors and thus the prediction maps still have much uncertainty.

Remote and proximal-sensors such ground penetrating radar (GPR) (Comas et al., 2015), electromagnetic induction (Altdorff et al., 2016), gamma radiometer (Rawlins et al., 2009; Keaney et al., 2013), and light detection and ranging (LiDAR) also have been proposed for mapping peat extent and thickness (Fyfe et al., 2014; Keaney et al., 2013; Koszinski et al., 2015; Parry et al., 2014; Rosa et al., 2009). These instruments produce high-resolution data; however, they still need ground data for calibration which may not be feasible in remote areas. Furthermore, the high cost of acquiring these data does not allow a wide application in large parts of Indonesia. In particular, airborne LiDAR has been proposed as a method to map fine resolution elevation and identify deep peat soils (peat domes) (Hooijer and Vernimmen, 2013). However, LiDAR only can infer peat domes and cannot delineate peat areas.

In a recent study, Rudiyanto et al. (2016b) proposed the digital soil mapping (DSM) framework (McBratney et al., 2003) widely used in the research community for mapping carbon in mineral soils (Minasny et al., 2013), as a cost-effective method for mapping peat thickness. They demonstrated successful applications in two peatlands in Sumatra and Kalimantan. In digital mapping, field observations are coupled with multi-source remotely-sensed environmental variables. This fusion of data allows the creation of spatial prediction functions via machine-learning algorithms. This produces an objective and accurate maps in the form of rasters of prediction along with the confidence of prediction. Consequently, they significantly improved the results of peat thickness mapping (in terms of better accuracy and resolution) as compared to previous studies (e.g. Jaenicke et al., 2008).

The main objective of this study is to propose and demonstrate an open digital mapping approach, which utilises open data in an open-source computing environment, as a cost-effective method for mapping Indonesian peatlands. We validate this approach in a study area in Bengkalis island, Riau province, Indonesia, with specific objectives:

- To evaluate the efficacy of various types of environmental covariates including elevation, terrain attributes, distance to rivers and or sea, radar and optical images for digital mapping of peat thickness,
- To evaluate the accuracy of various types of machine-learning models,
- To evaluate the effect of number of observations of peat thickness on the accuracy of the models,
- To map peat thickness accurately along with its prediction confidence, at a raster resolution of 30 m,
- To estimate below ground carbon stock along with its uncertainty, and
- To provide a relationship between accuracy, cost and time requirement for peat mapping.

2. Materials and methods

2.1. Study area

The study area is located in the eastern part of Bengkalis Island (Fig. 1a and b), Riau Province, Indonesia; which covers an area of around 50,000 ha at latitudes: N1.2502° to N1.5637° and longitudes: E102.2658° to E102.5087°. This area was provided by the Indonesian Peat Prize (IPP) committee as part of its test site. Peatland in Bengkalis island was previously studied by Supardi et al. (1993). Bengkalis island is about 10 km located off the east coast of the Riau province in the strait of Malacca. Its mean annual rainfall is 2400 mm and a mean annual temperature of 27 °C.

Carbon-14 dating showed that the accumulation of this Holocene peat range from 4740 ± 200 to 5730 ± 180 year B.P. (Supardi et al., 1993) when rising sea level stabilized, which resulted in exposure of large, relatively flat areas of marine sediments (Neuzil et al., 1993). The initial 3 m of peat accumulated rapidly at an average rate of 5.1 mm $year^{-1}$, and the upper 5 m of peat accumulated at a slower rate of 1.2 mm $year^{-1}$. The peat is ombrogenic, fibric-hemic to hemic-sapric. The main land use is forestry, with some areas planted with oil palm, and others used for dry land farming. Since 2012, there has been a large land use change with conversion of primary forests, and mangroves to industrial plantations (Barus et al., 2016).

2.2. Data set

2.2.1. Data set from field observation and laboratory measurements

Peat thickness was observed in the field using a Russian-type peat corer (Jowsey, 1966) along with their geographical coordinates with a handheld global positioning system (GPS).

117 observations were obtained from the Ministry of Environment and Forestry (MOEF) Indonesia that were collected in 2015. In addition, we collected additional field data in February 2017 to fill in the geographical gaps of existing data (n = 42). Thus, overall, 159 peat thickness observations were used in this study. Fig. 1b shows point locations of peat thickness measurements. The distribution of peat thickness for all data is shown in Fig. 2. Peat thickness ranges between 0 and 12 m with a median of 6.0 m.

We also collected 34 peat samples from the depth up to 30 cm in the 2017 survey for laboratory analysis. Bulk density (BD), carbon content (C_c) were measured on those samples at the Laboratory of Soil Science in Riau University. BD was collected using a ring sampler and determined gravimetrically. Organic matter content was determined using the loss on ignition (LOI) method and converted to C content using the van Bemmelen factor of 0.58. The plot of bulk density, BD vs. carbon content, C_c with their histogram is shown in Fig. S1 (Supplementary material). The data show that there is no relationship between C_c and BD. Observed bulk density ranges between 0.12 and 0.47 g cm^{-3} with a mean and SD of 0.226 ± 0.088 g cm^{-3}. Generally, the bulk density of tropical peat is between 0.013 and 0.25 g cm^{-3} (Rudiyanto et al., 2016a). Supardi et al. (1993) reported that an average bulk density of peatland in Bengkalis Island as 0.08 g cm^{-3}. Frizdew (2012) also showed a similar result of bulk density values obtained from Bengkalis for 0–1 m of depth which is equal to 0.074 ± 0.011 g cm^{-3}. Thus, the surface bulk density obtained in the field is relatively large, which may due to surface compaction. Observed carbon content varies between 0.498 and 0.578 g g^{-1} with a mean and SD of 0.568 ± 0.016 g g^{-1}. This is in accordance with values found in the literature for tropical peat where the C content values are between 0.5 and 0.62 g g^{-1} (Rudiyanto et al., 2016a). Supardi et al. (1993) showed relatively

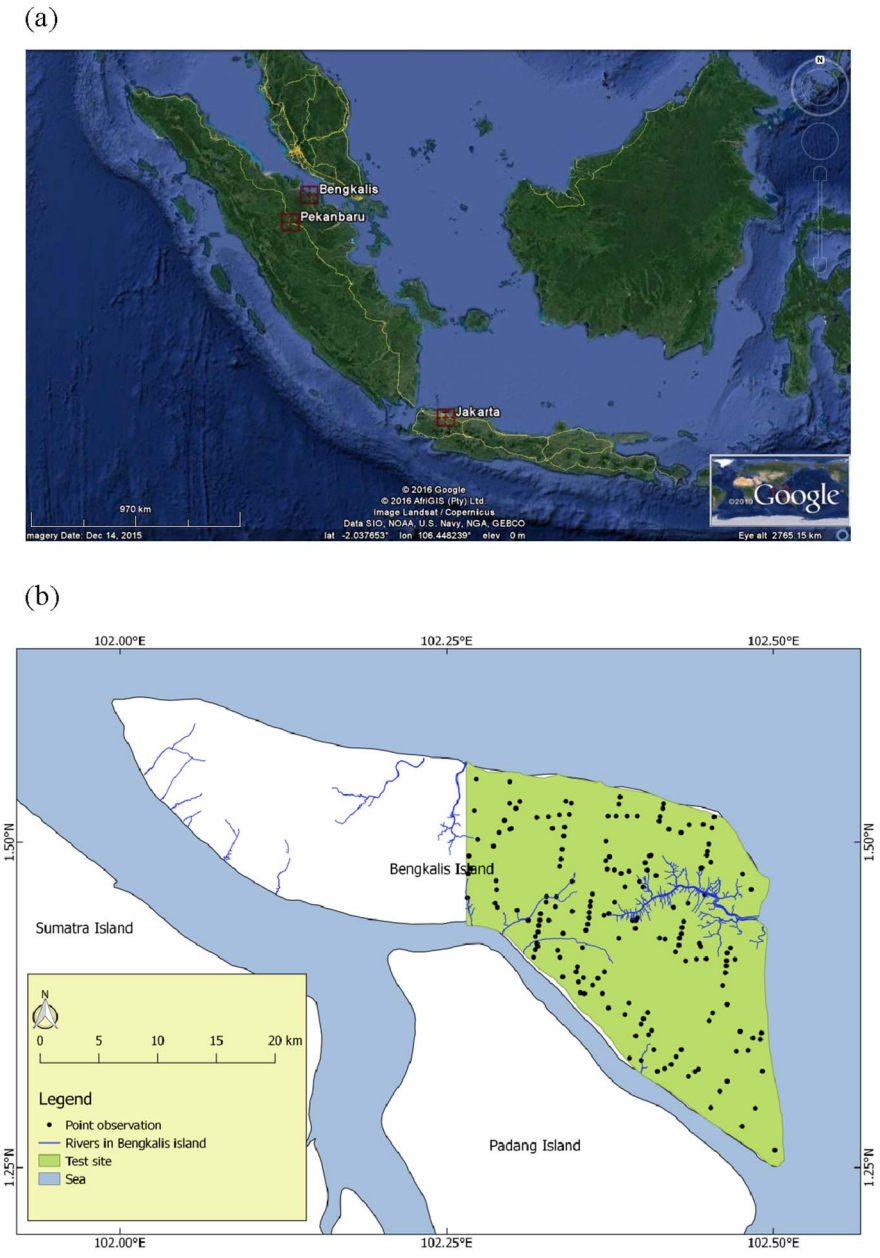

Fig. 1. (a) Location of Bengkalis Island and (b) test site (green colour). Symbols (black circles) are point observations of peat thickness. (For interpretation of the references to colour in this figure legend, the reader is referred to the web version of this article.)

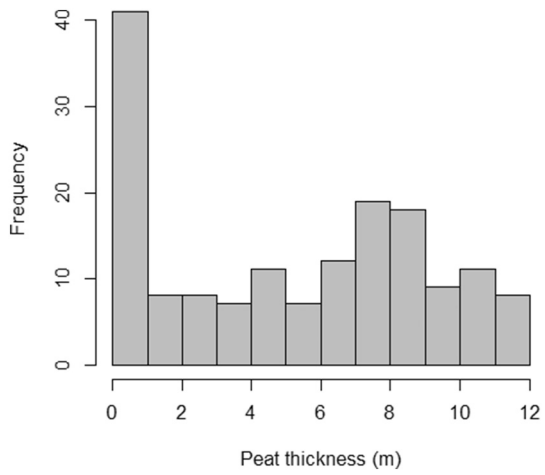

Fig. 2. Histogram of observed peat thickness (n = 159).

higher C contents in Bengkalis island which range between 0.604 and 0.630 g g^{-1} with an average of 0.619 g g^{-1}.

2.2.2. Multi-source environmental covariates

Here we used multi-source environmental data to model peat thickness. This is based on an adapted digital soil mapping (DSM) model of McBratney et al. (2003):

$$P = f(s, o, r, n), \quad (1)$$

where peat thickness (P) is a function of the surface or peat properties (s), organisms or plant or human activities (o), relief or topography (r), and spatial position (n). We assumed that other *scorpan* factors (climate, parent materials, and age) are constant within an area. We used a wide-range of data representing these factors, including SRTM DEM, terrain attributes, Landsat images, Radar images, and distances from rivers/sea.

2.2.2.1. Elevation and SRTM DEM correction. Rudiyanto et al. (2016b) found that elevation is the most important predictor in peat thickness

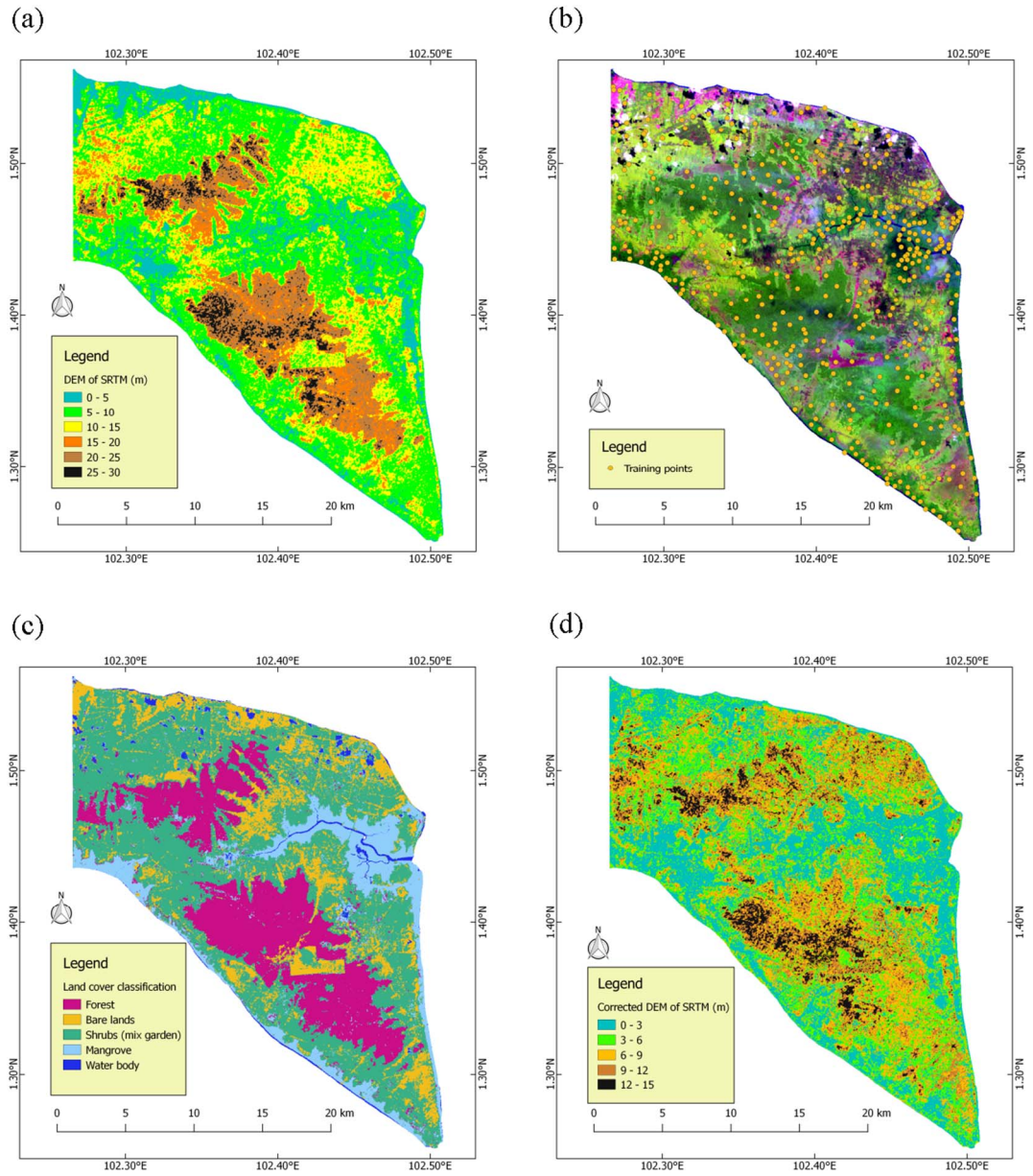

Fig. 3. The correction of SRTM DEM for vegetation. (a) Original SRTM DEM, (b) Landsat TM 5 with false composite colours (band 5, 4, 3), (d) land cover classification and (d) SRTM DEM corrected for vegetation height.

modelling since the surface of peatlands is convex where a peat dome is present (Anderson, 1964, 1961; Jaenicke et al., 2008). Peat can be very thick and concentrated in the dome (Esterle and Ferm, 1994).

The freely-available 1 arc-second DEM from the Shuttle Radar Topography Mission (SRTM) is often used for elevation modelling, however, the DEM includes vegetation height. Thus, we need to correct the SRTM DEM by subtracting corresponding vegetation height (O'Loughlin et al., 2016). We used the following basic approach:

- Land cover at the test site is first classified based on a cloud-free Landsat 5 Thematic Mapper (TM) image (Fig. 3b) that was acquired on 14 June 2000 since the SRTM DEM (Fig. 3a) was acquired in February 2000 (http://earthexplorer.usgs.gov/).
- Land cover types were classified into five groups including forest, bare land, shrubs (mix garden), mangrove and water body (Fig. 3c).
- Random forest classification algorithm was used to classify the Landsat image, where a training data (n = 1000) is randomly selected from the image (Fig. 3b). Nine environmental covariates were used including DEM of SRTM, Landsat 5 TM band 1–7, and Normalized Difference Vegetation Index calculated from Landsat, NDVI = (band 4 − band 3) / (band 4 + band 3) to predict the land cover type. The classification was conducted using the Random Forest (RF) algorithm in R (Liaw and Wiener, 2015, 2002).
- Naturally, vegetation heights vary spatially. However, since we do not have field measurements of tree height, we assumed that each of the land cover has a uniform vegetation height determined from representative sites at the boundary between bare and vegetated area. The height of the forest canopy is estimated at 13 m based on the DEM difference between forest and deforested area. Thus we provided an average vegetation height for bare land = 0 m, shrub (mix garden) = 5 m, mangrove = 4 m and water body = 0 m (Fig. 3c).
- SRTM DEM corrected for vegetation height (Fig. 3d) is obtained by subtracting vegetation height from the raw (or original) SRTM DEM.

Both the "original" SRTM DEM and vegetation corrected SRTM DEM

were tested as covariates in the modelling process.

2.2.2.2. Terrain attributes. From the corrected SRTM DEM, terrain attributes, namely multiresolution index of valley bottom flatness (MRVBF) and SAGA wetness index, were derived. MRVBF is a topographic index designed to identify areas of deposition at a range of scales (Gallant and Dowling, 2003). Flatness is measured from the inverse of slope, and lowness is measured from a ranking of elevation with respect to a circular surrounding area. The SAGA wetness index is an equivalent 'topographic wetness index' (TWI) which combines local upslope contributing area and slope, commonly used to quantify the topographic control on hydrological processes such as hydrological flow paths (Sørensen et al., 2006).

2.2.2.3. Distances to rivers and seas. Rudiyanto et al. (2016b) found that the Euclidean distance or the nearest distance to a river is another important factor in peat thickness modelling since rivers play an important role in peatland development (Anderson, 1964, 1961; Esterle and Ferm, 1994). Thus, we include the Euclidean distance to rivers as environmental covariates. Note that there are seven rivers in the test site (Fig. 1b). In addition to the nearest distance to rivers, the nearest distance to all rivers, sea and combined all rivers and sea were also tested.

2.2.2.4. Radar images. Two sets of radar data were used, i.e. Sentinel-1A (C-band synthetic aperture radar) and the phased array L-band synthetic aperture radar (PALSAR) on board the Advanced Land Observing Satellite (ALOS). Sentinel-1A dual-polarization VV and VH data were downloaded from two different sources: Google Earth Engine, GEE (https://earthengine.google.com/) and Alaska Satellite Facility (https://vertex.daac.asf.alaska.edu/#). ALOS-PALSAR from the year 2010 dual-polarization HH and HV data were obtained from the Alaska Satellite Facility (https://vertex.daac.asf.alaska.edu/#). In addition, we calculated the following indices from the dual-polarization data; the ratio (VV/VH), the mean value ((VV + VH) / 2) and the difference (VV − VH) for both Sentinel-1A and ALOS-PALSAR data. Radar images have been found useful in delineating wetland and peat areas (e.g. Kim et al., 2017; Mahdianpari et al., 2017).

2.2.2.5. Optical images. Optical images of Landsat 7 Enhanced Thematic Mapper Plus (ETM +) were downloaded from Google Earth Engine (https://earthengine.google.com/). A cloud-free image was selected as a composite from the year 2008–2012. Landsat 7 band 1 to 7 and its normalised difference vegetation index, NDVI were used as environmental covariates in this study as a proxy for vegetation and land cover.

In total, we ensembled 37 environmental covariates, which are listed in Table 1. The resolution for all raster covariates is 30 m except for Sentinel-1A from the Alaska Satellite Facility which has an original resolution of 11 m. The spatial resolution of Sentinel-1A from GEE has been aggregated to 30 m.

2.3. Variable selection

A large number of covariates (37), where some variables are correlated, can cause non-optimal solution for machine-learning algorithms. It addition, processing such a large amount of data (40 GB) require a lot of computer memory and computational time. Thus, we need to select only relevant covariates for peat thickness modelling and mapping. We used the variable selection algorithm, Boruta, available in an R package (Kursa and Rudnicki, 2010) as a feature selection method. Boruta works as a wrapper algorithm around Random Forest (Wright and Ziegler, 2017), where it finds relevant features by comparing the original covariates' importance with randomly permuted copies of the covariates (Kursa and Rudnicki, 2010).

2.4. Development of peat thickness models

A suite of machine-learning models was used to test if any particular model performs better in spatial prediction functions of peat thickness. Here, 14 machine-learning models were evaluated including Cubist (Kuhn et al., 2014), quantreg Forest: Quantile Regression Forests (QRF) (Meinshausen, 2006; Meinshausen and Schiesser, 2014), random forest (RF) (Liaw and Wiener, 2015, 2002), nnet (Venables and Ripley, 2002), neural networks using model averaging (avNNet) (Kuhn et al., 2012), bagging (Peters et al., 2017), Conditional Inference Trees (ctree) (Hothorn et al., 2006; Hothorn and Zeileis, 2015), evtree (Grubinger et al., 2014), gbm (Ridgeway, 2017), k-Nearest Neighbour Regression (knnreg) (Kuhn et al., 2012), partial least squares regression (PLSR) and principal component regression (PCR) (Mevik and Wehrens, 2007), regression tree rpart (Therneau et al., 2015) and support vector machine svm-radial (Meyer et al., 2013). The R packages and versions of the 14 models are listed in Table S1 (Supplementary material).

The k-fold cross-validation approach was used to determine the accuracy and uncertainty of the peat thickness models in this study. This approach divides randomly the observed data into k groups and then trains k models using all except one of the subsets where this left-aside subset for each model was used for testing (Aitkenhead, 2017). We used the 10-fold cross-validation which is repeated 10 times in a random fashion, and consequently, each machine-learning method yielded 10 × 10 = 100 models of peat thickness. The performances of the models during training and testing in the k-fold cross-validation procedure were evaluated using the coefficient of determination, R^2 and the root mean square error (RMSE), median absolute error (MAE) and median absolute relative error (MARE). RMSE is calculated from:

$$\mathrm{RMSE} = \sqrt{\frac{\sum_{i=1}^{n} (\mathrm{do}_i - \mathrm{dp}_i)^2}{n}} \tag{2}$$

where do and dp are the observed and predicted peat thickness, n is number of data.

MAE is calculated from:

$$\mathrm{MAE} = \mathrm{median}\ |\mathrm{do}_i - \mathrm{dp}_i|, \tag{3}$$

and MARE is calculated from:

$$\mathrm{MARE} = \mathrm{median}\frac{|\mathrm{do}_i - \mathrm{dp}_i|}{\mathrm{do}_i}. \tag{4}$$

All algorithms in this study were coded in an open-source statistical program R, https://www.r-project.org/ (R Development Core Team, 2008) using the RStudio interface (https://www.rstudio.com/).

2.5. Development of peat thickness map

The best machine-learning model was selected and the peat thickness map and its uncertainty were generated using the k-fold cross-validation (k = 10) technique with 5 realisations. This technique resulted in 10 × 5 = 50 realisation maps. We calculated the mean and standard deviation, μ ± σ of peat thickness for each raster cell (or every 30 m × 30 m). The 90% confidence interval was calculated using the relationship μ ± 1.645σ, assuming the distribution of predicted peat thickness is Gaussian. The R package Raster (Hijmans and van Etten, 2016) was used to generate peat thickness map from a raster set of covariates.

2.6. Calculation of peat volume, carbon stock and its uncertainty

2.6.1. Calculation of peat volume

Peat volume was calculated using the following equation:

$$V = A_{\mathrm{cell}} \sum_{i=1}^{n} d_i \tag{5}$$

where V is peat volume (m^3), d_i is peat thickness (m) at raster cell-i, A_{cell} is area of the raster cell which is equal to 30 × 30 m^2, and n is the number of the raster cell of peat thickness in the respective area.

2.6.2. Calculation of carbon stock

First, carbon density or organic carbon content by volume was calculated from carbon content and bulk density:

$$C_v = C_c \rho_b \quad (6)$$

where, C_v is organic carbon content by volume (in Mg m^{-3}), C_c is organic carbon content by mass (g of C/g of dry soil), and ρ_b is bulk density (in Mg m^{-3}). Carbon content and bulk density would vary with space and depth and can affect the estimates of carbon density as well as carbon stock. Since most deep tropical peat has a relative constant value of C content at 0.5501 ± 0.0225 g g^{-1} (Rudiyanto et al., 2016a) and the limited number of samples in this area, the average and standard deviation of carbon content and bulk density were used in calculation.

Finally, carbon stock for each pixel in the respective peatland was calculated using the following equation:

$$C_{stock} = C_v V \quad (7)$$

where, C_{stock} is carbon stock (tonne or Mg).

2.6.3. Uncertainty analysis

The rules of error propagation (e.g., Bevington and Robinson, 2002) were used to evaluate the uncertainty in the estimation of peat volume, organic content as well as carbon stock. The uncertainty for peat volume (Eq. (5)) estimate was calculated using the following equation:

$$\sigma_V^2 = A_{cell}^2 \sum_{i=1}^{n} (\sigma_{d_i}^2) \quad (8)$$

where, σ_v and σ_{di} are standard deviations (SD) for peat volume and peat thickness at raster cell-i, respectively.

The uncertainty for carbon density (Eq. (6)) was calculated using the following equation:

$$\left(\frac{\sigma_{C_v}}{C_v}\right)^2 = \left(\frac{\sigma_{C_c}}{C_c}\right)^2 + \left(\frac{\sigma_{\rho_b}}{\rho_b}\right)^2 \quad (9)$$

where, σ_{Cv} and σ_{Cc} and $\sigma_{\rho b}$ are standard deviations for C_v, C_c and ρ_b, respectively. This uncertainty calculation does not consider the correlation between C_c and ρ_b, as it was found the two variables were uncorrelated in tropical peats (Rudiyanto et al., 2016b).

Finally, the uncertainty for carbon stock (Eq. (7)) was calculated using the following equation:

$$\left(\frac{\sigma_{C_{stock}}}{C_{stock}}\right)^2 = \left(\frac{\sigma_{C_v}}{C_v}\right)^2 + \left(\frac{\sigma_V}{V}\right)^2 \quad (10)$$

where, σ_{Cstock} is standard deviation of C stock estimate (Mg).

3. Results and discussion

3.1. Peat thickness modelling

3.1.1. Variable selection

The data set of peat thickness (n = 159) was used to select relevant covariates using the R package Boruta. The result of variable selection is shown in Table 1. From 37 covariates, 18 covariates were confirmed (as relevant), 4 covariates were tentative and 13 covariates were rejected (see decision column in Table 1).

DEM corrected for vegetation shows a higher contribution to the model compared to the original DEM, which indicates that vegetation height correction is essential and the simple correction method works. Terrain attribute MRVBF derived from DEM is confirmed as a relevant predictor while topographic wetness index (TWI) is rejected as the peatland was developed in a relatively flat area.

Table 1
Environmental covariates for peat thickness mapping.

No	Environmental covariates	meanImp	Rank	Decision
1	*DEM of SRTM original*	12.0	3	Confirmed
2	**DEM of SRTM with vegetation correction**	15.5	1	Confirmed
3	**MRVBF of DEM of SRTM with veg. correction**	13.5	2	Confirmed
4	TWI of DEM of SRTM with veg. correction	1.7	26	Rejected
5	**Sentinel-1A VV from GEE**	10.5	4	Confirmed
6	Sentinel-1A VH from GEE	3.0	21	Tentative
7	**Sentinel-1A ratio between VV and VH from GEE**	9.5	5	Confirmed
8	**Sentinel-1A mean VV and VH from GEE**	7.5	9	Confirmed
9	Sentinel-1A VV minus VH from GEE	0.4	34	Rejected
10	*Sentinel-1A VV (2016) from Alaska Satellite Facility*	*3.7*	*17*	*Confirmed*
11	Sentinel-1A VH (2016) from Alaska Satellite Facility	0.9	30	Rejected
12	Sentinel-1A ratio between VV and VH (2016) from Alaska Satellite Facility	0.6	31	Rejected
13	Sentinel-1A mean VV and VH (2016) from Alaska Satellite Facility	1.9	25	Rejected
14	*Sentinel-1A VV minus VH (2016) from Alaska Satellite Facility*	*4.3*	*15*	*Confirmed*
15	*ALOS PALSAR HV (2010) from Alaska Satellite Facility*	*3.8*	*16*	*Confirmed*
16	**ALOS PALSAR HH (2010)**	6.7	11	Confirmed
17	*ALOS PALSAR ratio of HV and HH (2010)*	*3.6*	*18*	*Confirmed*
18	**ALOS PALSAR mean HV and HH (2010)**	6.3	12	Confirmed
19	**ALOS PALSAR HV minus HH (2010)**	7.0	10	Confirmed
20	Landsat 7 2008–2012 band 1 (blue)	1.7	27	Rejected
21	Landsat 7 2008–2012 band 2 (green)	0.3	35	Rejected
22	Landsat 7 2008–2012 band 3 (red)	0.4	33	Rejected
23	Landsat 7 2008–2012 band 4 (NIR)	0.5	32	Rejected
24	Landsat 7 2008–2012 band 5 (SWIR-1)	0.2	36	Rejected
25	Landsat 7 2008–2012 band 6 (TIR)	− 0.5	37	Rejected
26	Landsat 7 2008–2012 band 7 (SWIR-2)	1.0	29	Rejected
27	NDVI Landsat 7 2008–2012	2.2	24	Tentative
28	Euclidean distance to river 1	3.1	20	Tentative
29	**Euclidean distance to river 2**	3.2	19	Tentative
30	**Euclidean distance to river 3**	8.2	6	Confirmed
31	**Euclidean distance to river 4**	7.9	8	Confirmed
32	Euclidean distance to river 5	1.6	28	Rejected
33	**Euclidean distance to river 6**	2.8	22	Tentative
34	Euclidean distance to river 7	2.6	23	Tentative
35	**Euclidean distance to all rivers 1–7**	5.1	13	Confirmed
36	**Euclidean distance to sea**	4.7	14	Confirmed
37	**Euclidean distance to all rivers 1–7 and sea**	7.9	7	Confirmed

Radar images of Sentinel-1A from Google Earth Engine and its derivative (the VV and VH ratio, mean and difference values) show higher influences than the raw Sentinel-1A data obtained from Alaska Satellite Facility. The Sentinel-1A derived from Google Earth Engine has been pre-processed including filtering and aggregated to 30 m. Another radar image, ALOS PALSAR and its derivative (the HH and HV ratio, mean and difference values) are mostly confirmed as useful predictors although has lower contribution compared to Sentinel-1A.

All bands from Landsat 7 ETM + and its NDVI were rejected, indicating that land cover has no effect in the model which may due to high dynamic changes of land cover in the area. From 10 variables that are related to the Euclidean distance to rivers and/or sea, only one river (river-5) is rejected. This result shows the importance of rivers and or sea in peat development.

Based on the selection results, 15 variables (marked with bolt fonts in Table 1) including SRTM DEM with vegetation correction and its MRVBF, Sentinel-1A VV, VV/VH, (VV + VH) / 2 from GEE, ALOS PALSAR HH, (HH + HV) / 2, (HH − HV), and Euclidean distance to rivers 2, 3, 4, 6, all river, sea and all river and sea were used in peat thickness modelling. Note that the original SRTM DEM was excluded since elevation is already represented by SRTM DEM with vegetation correction. Furthermore, to

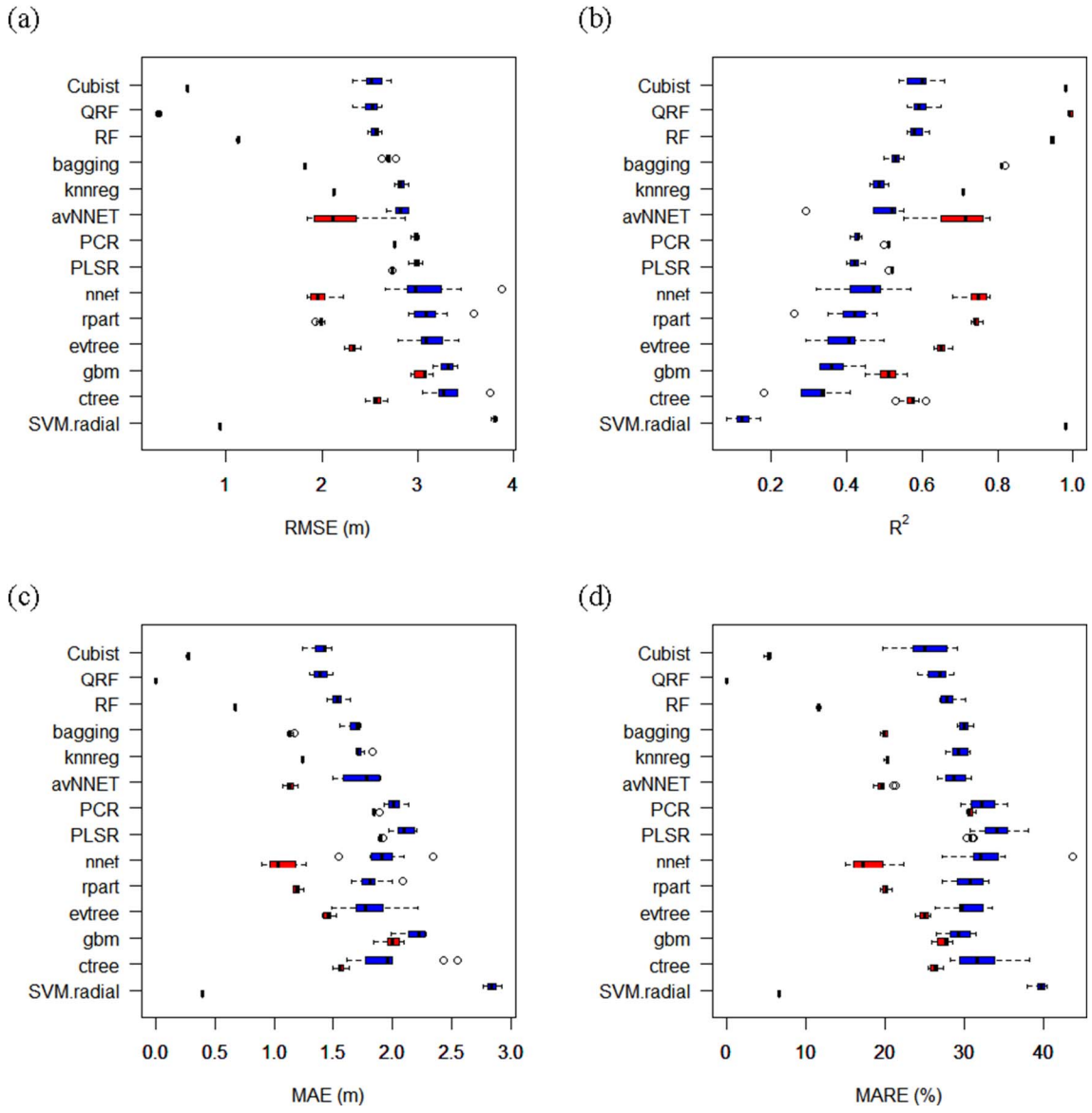

Fig. 4. Box plot of RMSE, R^2, MAE and MARE values of 14 regression models for predicting peat thickness. The blue colour is testing and red colour is training data from 10 realisations of 10-fold cross-validation. (For interpretation of the references to colour in this figure legend, the reader is referred to the web version of this article.)

simplify the model and reduce computational cost, Sentinel-1A VV, the difference of Sentinel-1A VV and VH, ALOS PALSAR HV and its band ratio which are the four lowest ranks were excluded. Although the status of Euclidean distance to rivers 2 and 6 are tentative, they were included since there is non-peatland around these two rivers and it may improve the model prediction. From these results, it is evident that peat thickness is not only related to elevation. Radar images, areas of deposition, and distance to the river are also highly relevant.

3.1.2. Model selection

The data of peat thickness observation (n = 159), and 15 selected environmental covariates from Section 3.1.1, were used to evaluate the performance of 14 machine-learning models. Based on the 10-fold cross-validation with 10 realisations, the results of indicator performances RMSE and R^2 for those 14 models are shown in Fig. 4. The best three models are Cubist, quantregForest (QRF), and randomForest (RF) having similar mean values of RMSE = 2.5 m, R^2 = 0.6, MAE = 1.4 m and MARE = 25% in testing. In calibration data, the performance of the 3 models is: RMSE = 0.6, 0.28 and 1.1 m; R^2 = 0.95, 0.99 and 0.98, MAE = 0.28, 0, and 0.67 m, respectively.

The agreement between observed and predicted peat thickness for those three models from one of the cross-validation realisation is shown in Fig. S2 (Supplementary material). In the testing data, all three models show a similar response where it slightly overestimates shallow or non-peat area and conversely underestimates deep peat. Fig. 7 also shows a large discrepancy between training and testing results for QRF (training MAE = 0), suggesting that QRF may overfit the training data.

All three models, Cubist, QRF and RF are typical tree-based ensemble method. This suggests that tree-based model performs better compared to other more continuous parametric models such as neural networks (ANN), support vector machine (SVM), partial least squares regression (PLSR), or simple linear regression model. We note that the covariates were selected using a wrapper around the randomforest algorithm (see Section 2.3) and therefore the selected covariates maybe optimised for these tree-based models.

The Cubist model, an advanced regression tree model produces a set of “if — then” rules, where each rule has an associated multivariate linear model. Whenever a set of covariates matches a rule's conditions, the associated model is used to calculate the predicted value. An example of such rule is:

Model 1:

Rule 1/1: [26 cases, mean 0.855, range 0 to 4.66, est err 0.918]

If

srtm_veg_cor <= 2.97531

then

outcome = -1.716 - 1506.8 ap_hh + 1493 ap_mean - 759.3 ap_minus
- 0.62 mrvbf_srtm_veg_cor + 0.15 srtm_veg_cor
- 7.1e-005 ed_river_3 - 5.4e-005 ed_river_6 - 0.44 sent1a_vv
+ 6.4e-005 ed_river_4 + 0.00011 ed_sea + 8 sent1a_div

where srtm_veg_cor is the DEM with vegetation correction, ap_hh is the ALOS PALSAR HH, ap_mean is the ALOS PALSAR mean of HV and HH, ap_minus is the ALOS PALSAR HV − HH, mrvbf_srtm_veg_cor is the MRVBF derived from corrected DEM, sent1a_vv is the Sentinel-1A VV, sent1a_div is the Sentinel-1A ratio between VV and VH, and ed_river_3, 4, 6 and sea are the distance to rivers 3, 4, 6 and sea, respectively.

3.1.3. Important variables for peat thickness mapping

One of the advantages of the tree-based models is that they provide a list of variables of importance in prediction. Fig. 5a and b shows variables of importance for Cubist and QRF, respectively. It shows that the top five important variables are vegetation corrected DEM and MRVBF, Sentinel-1A image and its indices. DEM (Fig. 3d) is related to peat dome where the deeper peat is generally located at higher elevation. MRVBF (Fig. 6a) is related to areas of peat deposition (green colour in the MRVBF map). Areas of large Sentinel-1A VV/VH values are related to wetter areas (Fig. 6b) which is in accordance with results from (Cazals et al., 2016; Muro et al., 2016). Both models show that the distance to river 3 is significant (Fig. 6c). ALOS PALSAR images (Fig. 6d) have low prediction importance compared to other covariates as the role of RADAR may already be captured by Sentinel images.

3.1.4. The effect of number observations on the accuracy of peat thickness modelling

The number of representative peat thickness samples is essential to generate an accurate peat thickness map in digital mapping. To evaluate the effect of the number of observations on the accuracy of peat thickness modelling, the Cubist tree model was used in a simulation. The available data (n = 159) were divided randomly into two groups: training and testing data set. Five scenarios with different number of training data were simulated and presented in Table 2. The model for each scenario was simulated 100 times and its performance was evaluated using Root Mean Square Error (RMSE), the coefficient of determination (R^2), median absolute error (MAE) and median absolute relative error (MARE).

Fig. 7 shows that the accuracy of the model increases (i.e. R^2 increases and or RMSE decreases) with the increasing number of training data. For 150 samples, the model can result in a range of R^2 of 0.5–0.7, RMSE = 1.80–2.80 m, MAE = 1–1.8 m, and MARE = 20–30%, respectively. Thus, we expect R^2 to increase to 0.6–0.7 when 200

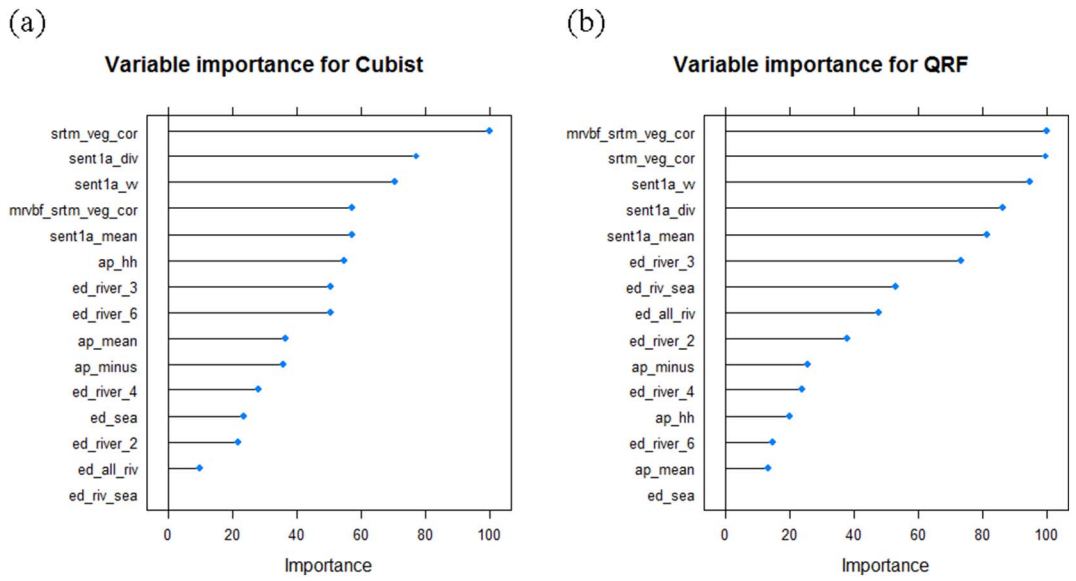

Fig. 5. Variable importance for (a) Cubist and (b) QRF in peat thickness modelling.

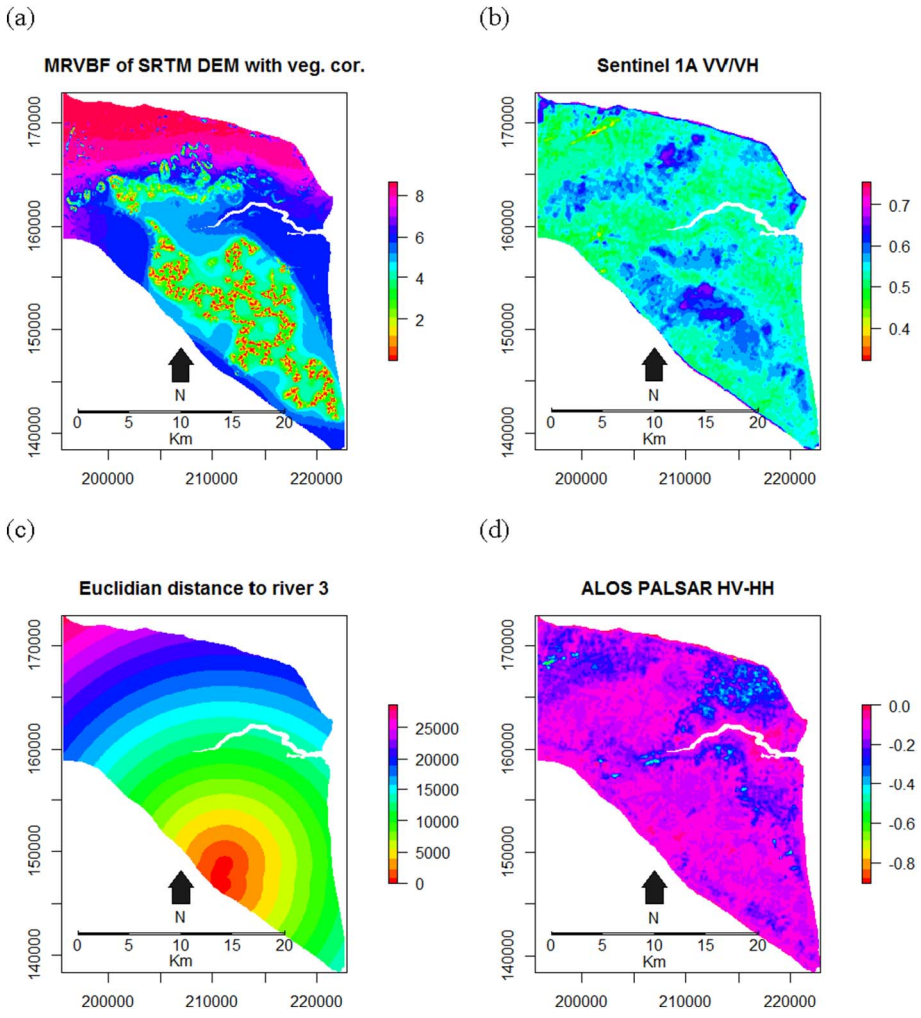

Fig. 6. Raster maps for (a) MRVBF of SRTM DEM with vegetation correction, (b) Sentinel 1A VV/VH, (c) Euclidean distance to river 3 and (d) ALOS PALSAR HV-HH.

Table 2
Five scenarios for different number of training and testing data.

Scenario	Number of data	
	Training	Testing
Ntr_50	50	109
Ntr_75	75	84
Ntr_100	100	59
Ntr_125	125	34
Ntr_150	150	9

observations are available. Thus, the accuracy of map results will depend on the number of point samples, thereby there is a tradeoff between accuracy and cost & time. This aspect will be further discussed in Section 3.5.

3.2. Peat thickness mapping

The best three regression models including Cubist, QRF and RF were selected as spatial predictive models for generating peat thickness map from 15 raster set of covariates (see variable selection section). Note that, waterbody especially of Kembung river (see Fig. 1b) was excluded

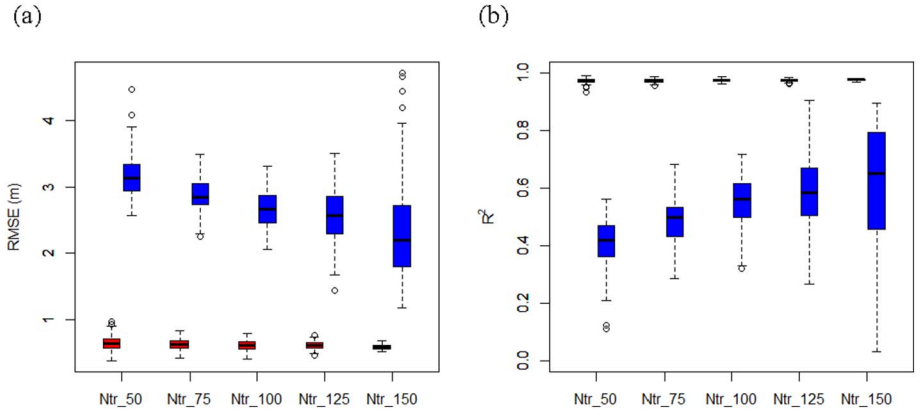

Fig. 7. (a) RMSE, (b) R^2, for five scenarios of different number of training (red) and testing (blue) data (Table 2) in peat thickness modelling. (For interpretation of the references to colour in this figure legend, the reader is referred to the web version of this article.)

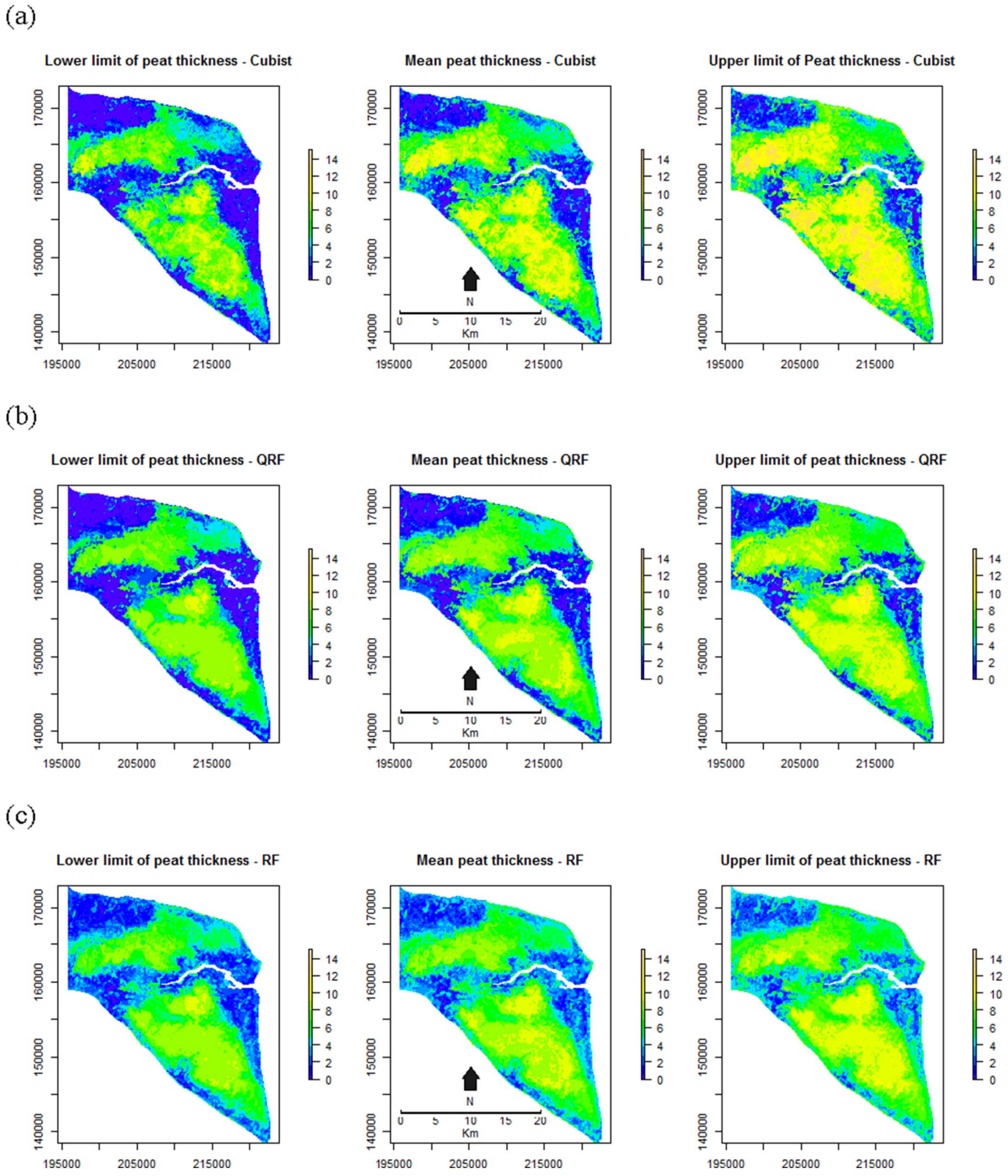

Fig. 8. Map of predicted peat thickness (mean with 90% confidence interval). (a) Cubist, (b) QRF and (c) RF.

from the map.

Predicted peat thickness maps (i.e., mean and its 90% confidence interval) using Cubist, QRF and RF models are presented in Fig. 8a, b and c, respectively. All maps show similar patterns with two hydrological peat units developed in southeast and west-south parts of test site-1. From k-fold cross validation, the Cubist model has R^2 = 0.93, RMSE = 0.92 m, and MARE = 12%, QRF with R^2 = 0.97, RMSE = 0.58 m, and MARE = 5% and RF with R^2 = 0.92, RMSE = 1.4 m, and MARE = 15% (see Fig. 9). It shows that the accuracy of maps is good.

While the performances of the three models are similar, the widths of the models' confidence intervals are different as shown in Table 3.

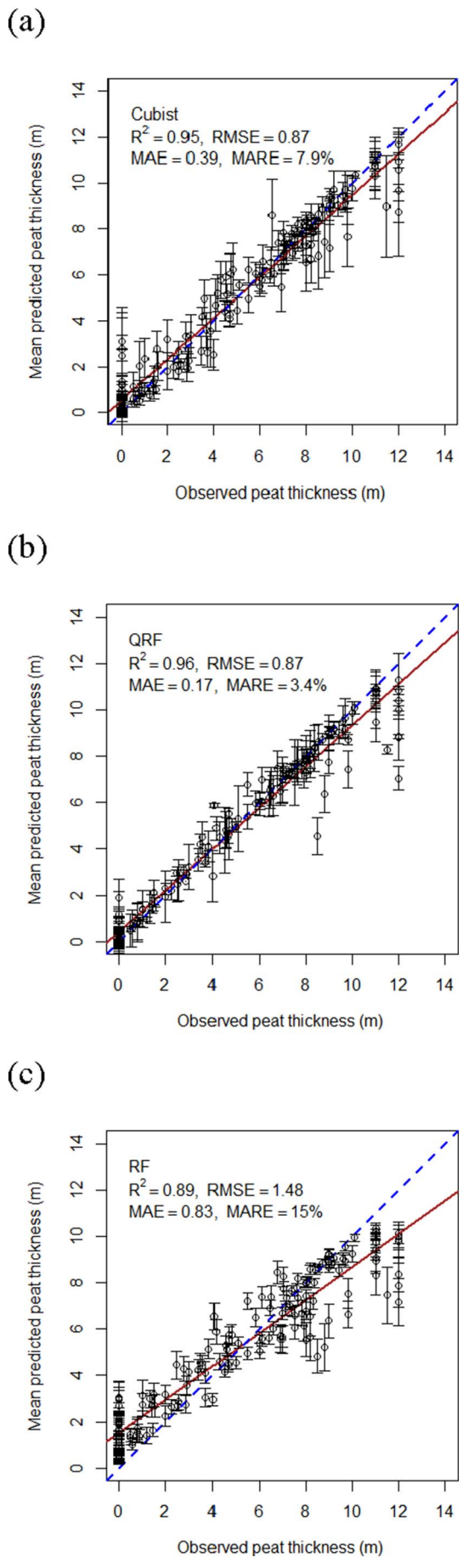

Fig. 9. The agreement between observed and predicted peat thickness at the observation points based on cross validation. The bar on each of the dots represents the 90% confidence interval. (a) Cubist, (b) QRF and (c) RF.

Table 3
Percentage of observed peat thickness, obs_pd (n = 159) that fall within the range of the lower and upper limits (CI 90%), as well as outside of lower and upper limits for Cubist, QRF and RF.

Inside	Outside	
Lower ≤ obs_pd ≤ upper	obs_pd < lower (overestimate)	obs_pd > upper (underestimate)
Cubist		
87%	6%	7%
QRF		
93%	1%	6%
RF		
24%	53%	33%

Table 4
The distribution of the peat area, volume and carbon stock over 15 classes of peat thickness from the peat thickness map that generated using the Cubist model.

Class	Depth range (m)	Area (ha)	Peat volume		C stock	
			Mean	SD	Mean	SD
			($\times 10^6$ m^3)		($\times 10^6$ t)	
0	≤ 0.5	3685	7.55	0.060	0.64	0.19
1	> 0.5–1	2404	18.00	0.094	1.53	0.46
2	> 1–2	4277	63.89	0.165	5.44	1.64
3	> 2–3	4131	102.84	0.188	8.76	2.64
4	> 3–4	3932	137.56	0.200	11.72	3.53
5	> 4–5	4262	192.35	0.208	16.39	4.94
6	> 5–6	4600	253.14	0.213	21.57	6.50
7	> 6–7	4960	322.95	0.214	27.52	8.29
8	> 7–8	4665	349.90	0.193	29.81	8.98
9	> 8–9	5691	484.74	0.185	41.30	12.44
10	> 9–10	6005	569.04	0.184	48.48	14.61
11	> 10–11	3211	334.73	0.141	28.52	8.59
12	> 11–12	965	109.51	0.086	9.33	2.81
13	> 12–13	72	8.81	0.027	0.75	0.23
14	> 13–14	1	0.12	0.003	0.01	0.003
	Total	52,861	2955.15	0.619*	251.8	75.87
	Water body	1273				

* Standard deviation of the total peat volume was calculated from Eq. (8).

The width of the 90% confidence interval (CI) in increasing order is as follow: RF < Cubist < QRF. We quantified the goodness of the uncertainty estimates using the percentage of observations that fall within the defined confidence interval (Vaysse and Lagacherie, 2017). Theoretically, 90% of the observations should fall within the prescribed interval. RF yielded the smallest uncertainty, however only about 24% of the observations fall in the defined 90% CI, implying it is overconfident. This is followed by Cubist where 87% of the observations fall in the CI and finally QRF where 93% of the observations fall in the CI. While the models performed similarly, Cubist and QRF produce the most reliable CI which was also reported by (Rudiyanto et al., 2016b).

3.3. Distribution of peat thickness area and calculation of belowground carbon stock and its uncertainty

3.3.1. Peat thickness map

The waterbody (about 1273 ha) is excluded from the peat map, and thus, in total, we mapped 52,861 ha from the total area of 54,133 ha. We grouped peat thickness into 15 classes from 0 to 0.5 m (which we considered as non-peat) to 14 m (the maximum predicted value) and

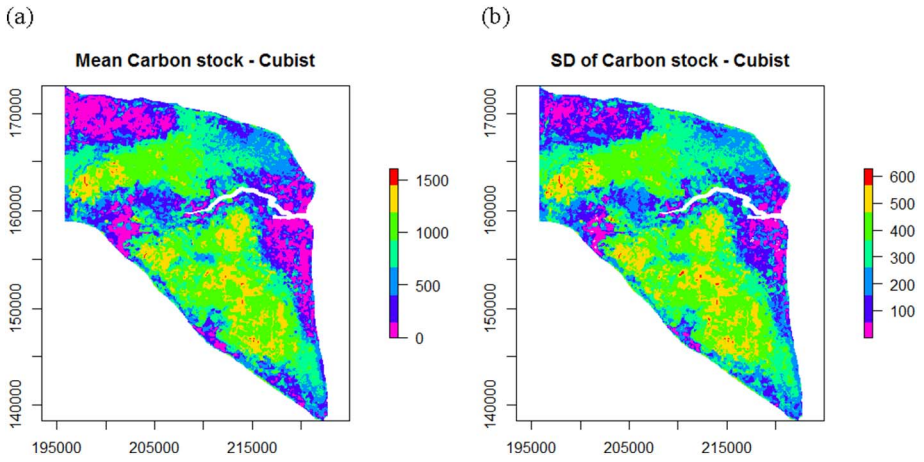

Fig. 10. (a) The mean and (b) standard deviation, SD of carbon stock maps that were generated using the Cubist model. Carbon stock unit is in tonne or Mg.

shown in Table 4. The area considered as mineral (non-peat) (depth 0–0.5 m) is 3685 ha (only 7% of the mapped area) while the rest is considered peat with an area of 49,176 ha. The total area considered as deep peat or conservation area (peat thickness > 3 m) is 38,364 ha (73% of the mapped area) and mostly peat is deposited at a thickness of 9–10 m (11% of the area).

We observed two peat domes with depth up to 10 m in the southeast and west-south parts of the study area (see Fig. 8). Similar maps were also produced by (Supardi, 1988) and the Ministry of Environment and Forestry (MOEF) Indonesia (MoEF, 2016).

3.3.2. Belowground C stock map

Digital maps consisting of the (a) mean and (b) standard deviation of peat thickness generated using the Cubist model is shown in Fig. S3 (Supplementary material). Based on the map of peat thickness and its uncertainty, the belowground C stock and its uncertainty can be calculated as follows. For each pixel:

- Determine the volume of peat (V in m^3) based on Eqs. (5) and (8).
- Estimate the average carbon density (C_v Mg m^{-3}) based on Eqs. (6) and (9). We used an average bulk density value from our data (0.226 ± 0.088 Mg m^{-3}) and Frizdew (2012) (0.074 ± 0.011 Mg m^{-3}), which is equal to 0.150 ± 0.045 Mg m^{-3}. The carbon content is equal to 0.568 ± 0.016 g g^{-1}. Assuming a normal distribution, the average carbon density, C_v and its standard deviation (SD) is 0.085 ± 0.026 Mg m^{-3} which is in line with the average carbon density of tropical peats (0.065 and 0.071 Mg m^{-3}) as reported by Warren et al. (2012) and Rudiyanto et al. (2016a) studies, respectively.
- Calculate carbon stock (C_{stock} in Mg) by multiplying the peat volume and C density ($V \times C_v$) using Eqs. (7) and (9).

Carbon stock for the whole area (in Mg) is calculated by summing the C stock for all pixels (excluding water bodies).

Maps of mean carbon stock and its standard deviation are shown in Fig. 10 and the distribution of carbon stock as well as its area and volume is presented in Table 4. It shows that the volume of peat in the study area is about 2955 ± 0.62 Mm^3 with a total carbon stock of 252 ± 76 Mt.

The method outlined above accounts both uncertainty in peat thickness mapping and C stock estimation. It improves over the current estimation methods which assume a constant peat thickness over the whole area (e.g. Page et al., 2011). This approach will reduce the C stock uncertainty calculation based on conventional soil maps (Warren et al., 2017).

3.4. Map production: accuracy, time and cost

3.4.1. Accuracy

In this study, the open digital mapping methodology was used to produce peat thickness map in a raster format with resolution 30 m or equivalent to a map of 1:30,000 scale covering a peatland area of 50,000 ha. Overall, 159 peat thickness observations were used to calibrate the advanced regression tree models. During calibration, the R^2 values are 0.98, with a median relative error of 5% and a median error of 0.3 m. From cross-validation, the model has an accuracy of R^2 of 0.5 to 0.7, RMSE = 1.8 to 2.8 m, a median relative error of 20 to 30% and a median error of 1 to 1.5 m. According to our simulation (Section 3.1.4), the accuracy will increase with increasing number of peat thickness observation. In addition, we describe the confidence of our prediction, which defines that 90% of the time the actual observations will fall into the prescribed limit.

3.4.2. Time

Based on our experience for the field survey in Bengkalis Island, two to five peat thickness observations can be obtained per day for a team of 4 surveyors. However, the effort will also depend on the access to location and peat thickness. Thus, for 150 observation points, it may take 1.5 to 2 months for one surveyor team.

If we wish to estimate the carbon stock, laboratory work is also

Table 5
Estimated accuracy, the time required and the cost of peat thickness mapping & C stock estimation at 30 m resolution for an area of 50,000 ha in Indonesia.

Number of samples (points)	Time required (months)	Accuracy		Cost			Total cost/ha (US $/ha)
		RMSE (m)	R^2 (–)	Field survey and laboratory work (US$)	Computer work (US$)	Total (US$)	
100	1–2	2.8	0.5	7500	5000	12,500	0.25
150	2–3	2.4	0.6	11,250	5000	16,250	0.30
200	2–3	2–2.4	0.6–0.7	15,000	5000	20,000	0.40
250	3–4	1.8–2.0	0.7–0.8	18,750	5000	23,750	0.50
Given	1	Depends on data			5000	5000	0.10

required for measurements of bulk density and carbon content. Alternatively, we can use published pedotransfer functions (Rudiyanto et al., 2016a).

Covariates are easily accessible from open-source data. All computer codes for digital mapping were developed in the free and open-source R software. Once field observations have been collected, the map can be easily generated.

3.4.3. Cost

The main cost for DSM is on field survey and computer processing. For field survey, the cost is for surveyors, transportation, accommodation, equipment use (peat auger, GPS, ring sample, etc.), and laboratory measurements. Based on this study, the cost for field survey and laboratory measurement is about Rp 1,000,000 (US $0.75) per sampling location. The cost for computer modelling and reporting is US$0.1/ha. This cost is for a trained digital soil mapper to collate covariates, writing codes, producing models, and generating map. The assumption is that the main parts of the code (intersecting observations and covariates, modelling using a defined algorithm, and producing maps) are already available.

Based on this result in the Bengkalis Island, we estimated the accuracy, time required and cost of peat thickness mapping and C stock estimation at a 30 m resolution in Table 5. The cost for mapping varies between $0.3 and $0.5/ha depending on the number of observations. The estimated time that required for these works (50,000 ha at a resolution of 30 m) is 2 to 4 months. Computer modelling is on a standard desktop computer (currently at a processing rate of 3 GHz and 8 GB RAM).

We note that:

- When data of peat thickness and their geographical coordinates are available; the cost is only for computer modelling at US$0.1/ha.
- For area > 1 million ha, the cost will be further reduced with an estimate of US$0.15 to $0.20/ha for a density of 1 to 2 observations/1000 ha. However, several groups of surveyors and programmers need to work in parallel in order to achieve a timely product.

3.4.4. Comparison with other methods

In term of cost, our open digital mapping methodology is significantly cheaper than conventional mapping and other technologies. Our method is 15 times cheaper than LiDAR acquisition that costs about $5 to $15/ha depending on the remoteness, size, accessibility and complexity of the area (e.g., Raison et al., 2015). LiDAR has been heavily promoted as the method for mapping peatland in Indonesia (Hooijer and Vernimmen, 2013). However, LiDAR only can identify deep, dome-shaped peat (convex) based on the assumption that the peat bottom is at the sea-level. As shown in this study, elevation is only one of several factors that governed the distribution of peat. Compared to the conventional mapping, our digital mapping is 3 to 4 times cheaper. As shown in many studies, digital mapping techniques are more accurate and more cost-effective than conventional mapping techniques (Minasny and McBratney, 2016; Zeraatpisheh et al., 2017).

3.5. Limitations and advantages of the digital mapping approach

We realise few limitations of our proposed method, i.e. it is based on empirical relationships between field observations and the covariates. Particularly, in this study area, field observations are based on existing samples which may be biased towards deeper peat areas. The measurement of thickness for the existing data set is rounded to the nearest 1 m, nevertheless our own data is measured to the nearest 1 cm. Peat thickness can vary with water table, and field measurements based on manual augering are only accurate up to 10 cm.

As this study area is dominated by peat, we modelled peat thickness for the whole area using a single model. For regional peat mapping, or areas with mixed mineral and peat soils, we need to first delineate the peat by generating a model of peat extent.

The covariates we used in this open approach are limited to open and freely available data. SRTM DEM can be affected by vegetation cover and may not be that accurate in lowland areas. Nevertheless, our method consistently shows that it can be used in lowland areas in Indonesia. The combination with other covariates proves that the method can be used extensively for mapping peatland. Currently there are also higher resolution Digital Terrain Model commercial products that are available globally, e.g. AW3D (5 m resolution) derived from JAXA-ALOS, and WorldDEM (12 resolution) from TanDEM-X Mission. Our preliminary testing did not show an advantage of using the 5 m AW3D DEM over the 30 m SRTM. The study by Samuel-Rosa et al. (2015) demonstrated that the use of more detailed or fine scale covariates only slightly improve the spatial prediction of soil properties. They further concluded that the modest increase in accuracy may not outweigh the extra costs of using more detailed covariates. Future work would compare the efficacy of various elevation covariates including LiDAR.

Digital soil mapping techniques have been successfully applied for nation-wide soil carbon mapping globally (e.g. national scale such as Kempen et al., 2009 in Netherlands; Adhikari et al., 2014 in Denmark; Akpa et al., 2016 in Nigeria; Grundy et al., 2015 in Australia, and Mulder et al., 2016 in France; Ramifehiarivo et al., 2017 in Madagascar; Poggio and Gimona, 2017 and Aitkenhead and Coull, 2016 in Scotland; Padarian et al., 2017 in Chile; and large regional scale such as Mansuy et al., 2014 in Canada; Tóth et al., 2017 and Ballabio et al., 2016 in Europe; Odgers et al., 2012 in USA). Thus to fulfill the need for a detailed national peat map, this study demonstrated many advantages of the open digital mapping method for peat thickness mapping and belowground carbon stock estimation:

- Evidence-based approach
  Digital soil mapping is an evidence-based approach, meaning that the method is derived from objective evidence of scientific research. It has been widely researched, compared with other methodologies, and extensively validated. It is therefore currently the best method from available scientific evidence.
- Open data
  All raster covariates (DEM SRTM, Sentinel-1A, ALOS PALSAR, etc.) can be obtained from public domain sites and can be downloaded freely. The generated peat thickness and C stock maps are in a common GIS raster format.
- Open-source and free software
  All procedures described here is documented in source codes written in an open-source and free software, R (https://www.r-project.org/), which is a popular language and environment for statistical computing and graphics. Additional (open-source) software tools such as SAGA (http://www.saga-gis.org/en/index.html) and QGIS (http://www.qgis.org/en/site/) are used especially in the pre-processing of covariates and map display. There is no third-party software which requires fees and licensing.
- Multi-source information
  Digital mapping techniques uses multiple sources of information from elevation, terrain attributes, radar, optical images, geographical locations and others. As peat development can be different between areas, this multitude of information can be adjusted and used in many places.
- Transparent algorithms
  All procedures in this approach are transparent. Machine-learning models that were used here such as Cubist, QRF, and RF are available in R packages have been tested by users from all over the world and the results have been recognised in peer-reviewed journals. There is no third-party or black box algorithm involved.
- Repeatable and Accountable
  The procedure in digital mapping can be repeated by other users and

applied in different areas, and thus all results are accountable.

- Flexible and can be readily updated (dynamic)
  With new data acquired, the map can be easily updated, and with new sensor data acquired in the area, e.g. better elevation and radar images, the maps can be easily updated.
- Accurate with confidence
  Digital mapping produces an accurate map, and in addition, defines the confidence of the prediction.
- Cost-effective and timely
  This is the most cost-effective method for mapping peat thickness over a large area in a timely manner. As long as the observations have been collected, the mapping process can be done efficiently using the latest computer technology.
- The ability to use existing observations
  Existing peat thickness observations collected by various government institutes and private sectors can be used to generate new high-resolution maps.
- Scalable to a national project
  Due to the open nature of the method (open data, open-source and transparent), the method is scalable and can be done in parallel by many groups in Indonesia. With appropriate training, various groups in Indonesia can perform this mapping procedure in a standard, and objective way. We envisage if done in parallel (both field work and computer modelling), utilising existing observations and collecting new observations, an accurate high-resolution peat maps (resolution of 30 m) for Indonesia can be done in 1.5–2 years.

4. Conclusions

This study demonstrated the open digital mapping approach as a cost-effective, timely, and accurate methodology for peat thickness mapping and carbon stock assessment in the Bengkalis island, Indonesia. In addition to the output of a raster map at a resolution of 30 m, it includes maps of the confidence of prediction. This is in response to the need of accurate peat maps for management and carbon conservation. Here we showed that:

- For the 50,000 hectare area, using 159 peat thickness observations, results show that our method can accurately predict peat thickness. Cross validation results showed that the median relative error is between 20 and 30%. The accuracy of the method can be further increased by increasing the number of field observations.
- Tree-based machine-learning models (i.e. Cubist, QRF and RF) are the best models.
- SRTM DEM with vegetation correction, and its MRVBF, Sentinel-1A radar images are the most important predictors of peat thickness. It confirms the importance of multi-source predictors in mapping peat thickness (Elevation, Radar, Rivers/Sea, and Optical).
- We tackle the issue of carbon stock calculation using an error propagation approach.
- The time required for the map production including field survey, laboratory measurement and computer work is 2 to 4 months with a cost about $0.3 to $0.5/ha. There is a tradeoff between cost and accuracy.

Finally, we highlighted the advantages of open digital mapping as an evidence-based, cost-effective and reliable method for mapping peat: open data, open-source and free software, multi-source data, transparent algorithms, repeatable and accountable, flexible and can be readily updated (dynamic), high accuracy with confidence, cost-effective and timely, the ability to use existing observations, and scalable to a national project. This flow work can be applied to any peatland in the world fulfilling the need for a national peatland map and belowground carbon stock estimation.

Acknowledgements

This study was part of our solution offered to the Indonesian Peat Prize (IPP) competition. The authors thanked Water Research Institute (WRI) Indonesia who organised the IPP event, gave financial support for field work, and provided the data set for this study. Wawan, Yan Gentara, Suryanto, and Irawan Dede Saputra from Faculty of Agriculture, Riau University (UNRI) helped in the field survey in Bengkalis island. The authors thank 2 anonymous reviewers for their constructive comments.

Appendix A. Supplementary data

Supplementary data to this article can be found online at https://doi.org/10.1016/j.geoderma.2017.10.018.

References

Adhikari, K., Hartemink, A.E., Minasny, B., Bou Kheir, R., Greve, M.B., Greve, M.H., 2014. Digital mapping of soil organic carbon contents and stocks in Denmark. PLoS One. http://dx.doi.org/10.1371/journal.pone.0105519.

Aitkenhead, M.J., 2017. Mapping peat in Scotland with remote sensing and site characteristics. Eur. J. Soil Sci. 68, 28–38. http://dx.doi.org/10.1111/ejss.12393.

Aitkenhead, M.J., Coull, M.C., 2016. Mapping soil carbon stocks across Scotland using a neural network model. Geoderma 262, 187–198. http://dx.doi.org/10.1016/j.geoderma.2015.08.034.

Akpa, S.I.C., Odeh, I.O.A., Bishop, T.F.A., Hartemink, A.E., Amapu, I.Y., 2016. Total soil organic carbon and carbon sequestration potential in Nigeria. Geoderma. http://dx.doi.org/10.1016/j.geoderma.2016.02.021.

Akumu, C.E., McLaughlin, J.W., 2014. Modeling peatland carbon stock in a delineated portion of the Nayshkootayaow river watershed in Far North, Ontario using an integrated GIS and remote sensing approach. Catena 121, 297–306. http://dx.doi.org/10.1016/j.catena.2014.05.025.

Altdorff, D., Bechtold, M., van der Kruk, J., Vereecken, H., Huisman, J.A., 2016. Mapping peat layer properties with multi-coil offset electromagnetic induction and laser scanning elevation data. Geoderma 261, 178–189. http://dx.doi.org/10.1016/j.geoderma.2015.07.015.

Anderson, J.A.R., 1961. The Ecology and Forest Types of the Peat Swamp Forests of Sarawak and Brunei in Relation to Their Silviculture. University of Edinburgh, Edinburgh, UK (PhD Thesis).

Anderson, J.A.R., 1964. The structure and development of the peat swamps of Sarawak and Brunei. J. Trop. Geogr. 18, 7–16.

Ballabio, C., Panagos, P., Monatanarella, L., 2016. Mapping topsoil physical properties at European scale using the LUCAS database. Geoderma 261, 110–123. http://dx.doi.org/10.1016/j.geoderma.2015.07.006.

Barus, B., Indraningsih, W., Purnama, A., HU, W., Iman, L., Yudarwati, R., 2016. Implication of peat land protection in Indonesia: a case study in Bengkalis Island, Riau. In: Advancing Inclusive Rural Development and Transformation in a Challenging Environment. UTM RAZAK SCHOOL of Engineering and Advanced Technology, Universiti Teknologi Malaysia, Kuala Lumpur, Malaysia, pp. 514.

Bauer, I.E., Gignac, L.D., Vitt, D.H., 2003. Development of a peatland complex in boreal western Canada: lateral site expansion and local variability in vegetation succession and long-term peat accumulation. Can. J. Bot. 81, 833–847. http://dx.doi.org/10.1139/b03-076.

Bevington, P.R., Robinson, D.K., 2002. Data Reduction and Error Analysis for the Physical Sciences, 3rd edition. McGraw-Hill Education, New York, USA.

Cazals, C., Rapinel, S., Frison, P.-L., Bonis, A., Mercier, G., Mallet, C., Corgne, S., Rudant, J.-P., 2016. Mapping and characterization of hydrological dynamics in a coastal marsh using high temporal resolution sentinel-1A images. Remote Sens. 8, 570. http://dx.doi.org/10.3390/rs8070570.

Comas, X., Terry, N., Slater, L., Warren, M., Kolka, R., Kristiyono, A., Sudiana, N., Nurjaman, D., Darusman, T., 2015. Imaging tropical peatlands in Indonesia using ground-penetrating radar (GPR) and electrical resistivity imaging (ERI): implications for carbon stock estimates and peat soil characterization. Biogeosciences 12, 2995–3007. http://dx.doi.org/10.5194/bg-12-2995-2015.

Comeau, L.-P., Hergoualc'h, K., Hartill, J., Smith, J., Verchot, L.V., Peak, D., Salim, A.M., 2016. How do the heterotrophic and the total soil respiration of an oil palm plantation on peat respond to nitrogen fertilizer application? Geoderma 268, 41–51. http://dx.doi.org/10.1016/j.geoderma.2016.01.016.

Draper, F.C., Roucoux, K.H., Lawson, I.T., Mitchard, E.T., Coronado, E.N.H., Lähteenoja, O., Montenegro, L.T., Sandoval, E.V., Zaráte, R., Baker, T.R., 2014. The distribution and amount of carbon in the largest peatland complex in Amazonia. Environ. Res. Lett. 9 (12), 124017.

Esterle, J.S., Ferm, J.C., 1994. Spatial variability in modern tropical peat deposits from Sarawak, Malaysia and Sumatra, Indonesia: analogues for coal. Int. J. Coal Geol. 26, 1–41. http://dx.doi.org/10.1016/0166-5162(94)90030-2.

Frizdew, R., 2012. Variasi kadar karbon organik berdasarkan perbedaan kedalaman muka air pada lahan gambut yang diusahakan untuk komoditas perkebunan. Institut Pertanian Bogor, Bogor, Indonesia (PhD thesis, in Bahasa Indonesia).

Fyfe, R.M., Coombe, R., Davies, H., Parry, L., 2014. The importance of sub-peat carbon storage as shown by data from Dartmoor, UK. Soil Use Manag. 30, 23–31. http://dx.doi.org/10.1111/sum.12091.

Gallant, J.C., Dowling, T.I., 2003. A multiresolution index of valley bottom flatness for

mapping depositional areas. Water Resour. Res. 39. http://dx.doi.org/10.1029/2002WR001426.
Grubinger, T., Zeileis, A., Pfeiffer, K.-P., 2014. Evtree: evolutionary learning of globally optimal classification and regression trees in R. J. Stat. Softw. http://dx.doi.org/10.18637/jss.v061.i01.
Grundy, M.J., Viscarra Rossel, R.A., Searle, R.D., Wilson, P.L., Chen, C., Gregory, L.J., 2015. Soil and landscape grid of Australia. Soil Res. 53, 835–844. http://dx.doi.org/10.1071/SR15191.
Hijmans, R.J., van Etten, J., 2016. raster: Geographic Data Analysis and Modeling. (R package version 2.5-8).
Holden, N.M., Connolly, J., 2011. Estimating the carbon stock of a blanket peat region using a peat depth inference model. Catena 86, 75–85. http://dx.doi.org/10.1016/j.catena.2011.02.002.
Hooijer, A., Vernimmen, R., 2013. Peatland maps for Indonesia. Including accuracy assessment and recommendations for improvement, elevation mapping and evaluation of future flood risk. In: Quick Assessment and Nationwide Screening (QANS) of Peat and Lowland Resources and Action Planning for the Implementation of a National Lowland Strategy. BAPPENAS & Ditjen Sumber Daya Air, Government of Indonesia & Partners for Water Programme, The Netherlands.
Hothorn, T., Zeileis, A., 2015. partykit: a toolkit for recursive partytioning. J. Mach. Learn. Res. 16, 3905–3909.
Hothorn, T., Hornik, K., Zeileis, A., 2006. Unbiased recursive partitioning: a conditional inference framework. J. Comput. Graph. Stat. 15, 651–674. http://dx.doi.org/10.1198/106186006X133933.
ICCC, 2014. ICCC Peatland Definition and Peatland Mapping Methodology Assessment Report. (Jakarta, Indonesia).
Jaenicke, J., Rieley, J.O., Mott, C., Kimman, P., Siegert, F., 2008. Determination of the amount of carbon stored in Indonesian peatlands. Geoderma 147, 151–158. http://dx.doi.org/10.1016/j.geoderma.2008.08.008.
Jowsey, P.C., 1966. An improved peat sampler. New Phytol. 65 (2), 245–248.
Keaney, A., McKinley, J., Graham, C., Robinson, M., Ruffell, A., 2013. Spatial statistics to estimate peat thickness using airborne radiometric data. Spat. Stat. 5, 3–24. http://dx.doi.org/10.1016/j.spasta.2013.05.003.
Kempen, B., Brus, D.J., Heuvelink, G.B.M., Stoorvogel, J.J., 2009. Updating the 1:50,000 Dutch soil map using legacy soil data: a multinomial logistic regression approach. Geoderma 151, 311–326. http://dx.doi.org/10.1016/j.geoderma.2009.04.023.
Kim, J.-W., Lu, Z., Gutenberg, L., Zhu, Z., 2017. Characterizing hydrologic changes of the Great Dismal Swamp using SAR/InSAR. Remote Sens. Environ. 198, 187–202. http://dx.doi.org/10.1016/j.rse.2017.06.009.
Koszinski, S., Miller, B.A., Hierold, W., Haelbich, H., Sommer, M., 2015. Spatial modeling of organic carbon in degraded peatland soils of Northeast Germany. Soil Sci. Soc. Am. J. 79, 1496–1508. http://dx.doi.org/10.2136/sssaj2015.01.0019.
Kuhn, M., Wing, J., Weston, S., Williams, A., Keefer, C., Engelhardt, A., 2012. Caret: classification and regression training. https://Cran.R-Project.Org/Package=Caret.
Kuhn, M., Weston, S., Keefer, C., Coulter, N., Quinlan, R., 2014. Cubist: Rule- and Instance-based Regression Modeling. (R package version 0.0.18).
Kursa, M.B., Rudnicki, W.R., 2010. Feature selection with the Boruta package. J. Stat. Softw. 36. http://dx.doi.org/10.18637/jss.v036.i11.
Liaw, A., Wiener, M., 2002. Classification and regression by randomForest. R News 2, 18–22.
Liaw, A., Wiener, M., 2015. Package 'randomForest'. Breiman and Cutler's random forests for classification and regression. In: CRAN Reference Manual.
Mahdianpari, M., Salehi, B., Mohammadimanesh, F., Motagh, M., 2017. Random forest wetland classification using ALOS-2 L-band, RADARSAT-2 C-band, and TerraSAR-X imagery. ISPRS J. Photogramm. Remote Sens. 130, 13–31. http://dx.doi.org/10.1016/j.isprsjprs.2017.05.010.
Mansuy, N., Thiffault, E., Paré, D., Bernier, P., Guindon, L., Villemaire, P., Poirier, V., Beaudoin, A., 2014. Digital mapping of soil properties in Canadian managed forests at 250 m of resolution using the k-nearest neighbor method. Geoderma 235, 59–73. http://dx.doi.org/10.1016/j.geoderma.2014.06.032.
McBratney, A., Mendonça Santos, M., Minasny, B., 2003. On digital soil mapping. Geoderma 117, 3–52. http://dx.doi.org/10.1016/S0016-7061(03)00223-4.
Meinshausen, N., 2006. Quantile regression forests. J. Mach. Learn. Res. 7, 983–999. http://dx.doi.org/10.1111/j.1541-0420.2010.01521.x.
Meinshausen, N., Schiesser, L., 2014. quantregForest: Quantile Regression Forests.
Mevik, B.-H., Wehrens, R., 2007. The pls package: principal component and partial least squares regression in R. J. Stat. Softw. http://dx.doi.org/10.1002/wics.10.
Meyer, D., Hornik, K., Weingessel, A., Leisch, F., Davidmeyerr-projectorg, M.D.M., 2013. Package "e1071". (E1071).
Minasny, B., McBratney, A.B., 2016. Digital soil mapping: a brief history and some lessons. Geoderma 264, 301–311. http://dx.doi.org/10.1016/j.geoderma.2015.07.017.
Minasny, B., McBratney, A.B., Malone, B.P., Wheeler, I., 2013. Digital mapping of soil carbon. Adv. Agron. 118, 1–47. http://dx.doi.org/10.1016/B978-0-12-405942-9.00001-3.
Mitra, S., Wassmann, R., Vlek, P.L.G., 2005. An appraisal of global wetland area and its organic carbon stock. Curr. Sci. 88, 25–35.
MoEF, 2016. Peta induktif penetapan fungsi dan fungsi budidaya ekosistem gambut. Kementerian lingkungan hidup dan kehutanan Republik Indonesia, Jakarta, Indonesia.
Mulder, V.L., Lacoste, M., Richer-de-Forges, A.C., Martin, M.P., Arrouays, D., 2016. National versus global modelling the 3D distribution of soil organic carbon in mainland France. Geoderma. http://dx.doi.org/10.1016/j.geoderma.2015.08.035.
Muro, J., Canty, M., Conradsen, K., Hüttich, C., Nielsen, A.A., Skriver, H., Remy, F., Strauch, A., Thonfeld, F., Menz, G., 2016. Short-term change detection in wetlands using Sentinel-1 time series. Remote Sens. 8 (10), 795. http://dx.doi.org/10.3390/rs8100795.
Neuzil, S.G., Supardi, Cecil, C.B., Kane, J.S., Soedjono, K., 1993. Inorganic geochemistry of domed peat in Indonesia and its implication for the origin of mineral matter in coal. Geol. Soc. Am. Spec. Pap. 286, 23–44. http://dx.doi.org/10.1130/SPE286-p23.
Odgers, N.P., Libohova, Z., Thompson, J.A., 2012. Equal-area spline functions applied to a legacy soil database to create weighted-means maps of soil organic carbon at a continental scale. Geoderma 189, 153–163. http://dx.doi.org/10.1016/j.geoderma.2012.05.026.
O'Loughlin, F.E., Paiva, R.C.D., Durand, M., Alsdorf, D.E., Bates, P.D., 2016. A multi-sensor approach towards a global vegetation corrected SRTM DEM product. Remote Sens. Environ. 182, 49–59. http://dx.doi.org/10.1016/j.rse.2016.04.018.
Padarian, J., Minasny, B., McBratney, A.B., 2017. Chile and the Chilean soil grid: a contribution to GlobalSoilMap. Geoderma Reg. 9, 17–28. http://dx.doi.org/10.1016/j.geodrs.2016.12.001.
Page, S.E., Rieley, J.O., Banks, C.J., 2011. Global and regional importance of the tropical peatland carbon pool. Glob. Chang. Biol. 17, 798–818. http://dx.doi.org/10.1111/j.1365-2486.2010.02279.x.
Parry, L.E., Charman, D.J., Noades, J.P.W., 2012. A method for modelling peat depth in blanket peatlands. Soil Use Manag. 28, 614–624. http://dx.doi.org/10.1111/j.1475-2743.2012.00447.x.
Parry, L.E., West, L.J., Holden, J., Chapman, P.J., 2014. Evaluating approaches for estimating peat depth. J. Geophys. Res. Biogeosci. 119, 2013JG002411. http://dx.doi.org/10.1002/2013JG002411.
Peters, A., Hothorn, T., Ripley, B.D., Therneau, T., Atkinson, B., 2017. ipred: Improved Predictors.
Poggio, L., Gimona, A., 2017. Assimilation of optical and radar remote sensing data in 3D mapping of soil properties over large areas. Sci. Total Environ. 579, 1094–1110. http://dx.doi.org/10.1016/j.scitotenv.2016.11.078.
Proulx-McInnis, S., St-Hilaire, A., Rousseau, A.N., Jutras, S., 2013. A review of ground-penetrating radar studies related to peatland stratigraphy with a case study on the determination of peat thickness in a northern boreal fen in Quebec, Canada. Prog. Phys. Geogr. 37, 67–786.
R Development Core Team, 2008. R: A language and environment for statistical computing. In: R Foundation for Statistical Computing. Vienna, Austria (ISBN 3-900051-07-0). http://www.R-project.org.
Raison, J., Atkinson, P., Chave, J., DeFries, R., Goh, K.J., Joosten, H., Navratil, P., Siegert, F., 2015. The High Carbon Stock Science Study: Independent Report From the Technical Committe. The High Carbon Stock Science Study, Kuala Lumpur.
Ramifehiarivo, N., Brossard, M., Grinand, C., Andriamananjara, A., Razafimbelo, T., Rasolohery, A., Razafimahatratra, H., Seyler, F., Ranaivoson, N., Rabenarivo, M., Albrecht, A., Razafindrabe, F., Razakamanarivo, H., 2017. Mapping soil organic carbon on a national scale: towards an improved and updated map of Madagascar. Geoderma Reg. 9, 29–38. http://dx.doi.org/10.1016/j.geodrs.2016.12.002.
Rawlins, B.G., Marchant, B.P., Smyth, D., Scheib, C., Lark, R.M., Jordan, C., 2009. Airborne radiometric survey data and a DTM as covariates for regional scale mapping of soil organic carbon across Northern Ireland. Eur. J. Soil Sci. 60, 44–54. http://dx.doi.org/10.1111/j.1365-2389.2008.01092.x.
Ridgeway, G., 2017. gbm: Generalized Boosted Regression Models.
Ritung, S., Wahyunto, Nugroho, K., Sukarman, Hikmatullah, Suparto, Tafakresnanto, C., 2011. Peta Lahan Gambut Indonesia Skala 1:250.000 (Indonesian Peatland Map at the Scale 1:250,000). The Ministry of Agriculture of Indonesia, Bogor, Indonesia.
Rosa, E., Larocque, M., Pellerin, S., Gagné, S., Fournier, B., 2009. Determining the number of manual measurements required to improve peat thickness estimations by ground penetrating radar. Earth Surf. Process. Landf. 34, 377–383. http://dx.doi.org/10.1002/esp.1741.
Rudiyanto, Setiawan, B.I., Arief, C., Saptomo, S.K., Gunawan, A., Kuswarman, Sungkono, Indriyanto, H., 2015. Estimating distribution of carbon stock in tropical peatland using a combination of an empirical peat depth model and GIS. Procedia Environ Sci 24, 152–157. http://dx.doi.org/10.1016/j.proenv.2015.03.020.
Rudiyanto, Minasny, B., Setiawan, B.I., 2016a. Further results on comparison of methods for quantifying soil carbon in tropical peats. Geoderma 269, 108–111. http://dx.doi.org/10.1016/j.geoderma.2016.01.038.
Rudiyanto, Minasny, B., Setiawan, B.I., Arif, C., Saptomo, S.K., Chadirin, Y., 2016b. Digital mapping for cost-effective and accurate prediction of the depth and carbon stocks in Indonesian peatlands. Geoderma 272, 20–31. http://dx.doi.org/10.1016/j.geoderma.2016.02.026.
Samuel-Rosa, A., Heuvelink, G.B.M., Vasques, G.M., Anjos, L.H.C., 2015. Do more detailed environmental covariates deliver more accurate soil maps? Geoderma. http://dx.doi.org/10.1016/j.geoderma.2014.12.017.
Shimada, S., Takada, M., Takahashi, H., 2016. Peat mapping. In: Osaki, M., Tsuji, N. (Eds.), Tropical Peatland Ecosystems. Springer Japan, Tokyo, pp. 455–467. http://dx.doi.org/10.1007/978-4-431-55681-7_31.
Sørensen, R., Zinko, U., Seibert, J., 2006. On the calculation of the topographic wetness index: evaluation of different methods based on field observations. Hydrol. Earth Syst. Sci. 10, 101–112. http://dx.doi.org/10.5194/hess-10-101-2006.
Supardi, 1988. Endapan Gambut Di Pulau Bengkalis Riau. Ministry of Energy and Mineral Resources of Indonesia, Bandung, Indonesia.
Supardi, Subekty, A.D., Neuzil, S.G., 1993. General geology and peat resources of the Siak Kanan and Bengkalis Island peat deposits, Sumatra, Indonesia. In: Modern and Ancient Coal-forming Environments, http://dx.doi.org/10.1130/SPE286-p45.
Therneau, T., Atkinson, B., Ripley, B., Ripley, M.B., 2015. rpart: Recursive Partitioning and Regression Trees. (R package version 4.1-10).
Tóth, B., Weynants, M., Pásztor, L., Hengl, T., 2017. 3D soil hydraulic database of Europe at 250 m resolution. Hydrol. Process. 31, 2662–2666. http://dx.doi.org/10.1002/hyp.11203.
van Bellen, S., Dallaire, P.-L., Garneau, M., Bergeron, Y., 2011. Quantifying spatial and temporal Holocene carbon accumulation in ombrotrophic peatlands of the Eastmain region, Quebec, Canada. Glob. Biogeochem. Cycles 25, GB2016. http://dx.doi.org/10.1029/2010GB003877.
Vaysse, K., Lagacherie, P., 2017. Using quantile regression forest to estimate uncertainty of digital soil mapping products. Geoderma 291, 55–64. http://dx.doi.org/10.1016/j.geoderma.2016.12.017.
Venables, W.N., Ripley, B.D., 2002. Modern Applied Statistics With S, fourth ed. Springer, New York. http://dx.doi.org/10.2307/2685660.
Wahyunto, R.S., Subagjo, H., 2003. Maps of Area of Peatland Distribution and Carbon Content in Sumatera, 1990–2002. Wetlands International – Indonesia Programme & Wildlife Habitat Canada (WHC).
Wahyunto, R.S., Subagjo, H., 2004. Map of Peatland Distribution Area and Carbon

Content in Kalimantan, 2000–2002. Wetlands International – Indonesia Programme & Wildlife Habitat Canada (WHC).
Wahyunto, R.S., Heryanto, B., Bekti, H., Widiastuti, F., 2006. Map of Peatland Distribution Area and Carbon Content in Papua, 2000–2001. Wetlands International – Indonesia Programme & Wildlife Habitat, Canada (WHC).
Warren, M.W., Kauffman, J.B., Murdiyarso, D., Anshari, G., Hergoualc'h, K., Kurnianto, S., Purbopuspito, J., Gusmayanti, E., Afifudin, M., Rahajoe, J., Alhamd, L., Limin, S., Iswandi, A., 2012. A cost-efficient method to assess carbon stocks in tropical peat soil. Biogeosciences 9, 4477–4485. http://dx.doi.org/10.5194/bg-9-4477-2012.
Warren, M., Hergoualc'h, K., Kauffman, J.B., Murdiyarso, D., Kolka, R., 2017. An appraisal of Indonesia's immense peat carbon stock using national peatland maps: uncertainties and potential losses from conversion. Carbon Balance Manag. 12, 12. http://dx.doi.org/10.1186/s13021-017-0080-2.
Weissert, L.F., Disney, M., 2013. Carbon storage in peatlands: a case study on the Isle of Man. Geoderma 204–205, 111–119. http://dx.doi.org/10.1016/j.geoderma.2013.04.016.
Wright, M.N., Ziegler, A., 2017. ranger: a fast implementation of random forests for high dimensional data in C++ and R. J. Stat. Softw. http://dx.doi.org/10.18637/jss.v077.i01.
Zeraatpisheh, M., Ayoubi, S., Jafari, A., Finke, P., 2017. Comparing the efficiency of digital and conventional soil mapping to predict soil types in a semi-arid region in Iran. Geomorphology 285, 186–204. http://dx.doi.org/10.1016/j.geomorph.2017.02.015.